

Hybrid Multi-Bernoulli and CPHD Filters for Superpositional Sensors

SANTOSH NANNURU

MARK COATES, Senior Member, IEEE
McGill University
Montreal, Canada

In this paper we present an approximate multi-Bernoulli filter and an approximate hybrid multi-Bernoulli cardinalized probability hypothesis density filter for superpositional sensors. The approximate-filter equations are derived by assuming that the predicted and posterior multitarget states have the same form and propagating the probability hypothesis density function for each independent component of the multitarget state. We examine the performance of the filters in a simulated acoustic sensor network and a radio frequency tomography application.

Manuscript received May 2, 2014; revised March 1, 2015; released for publication May 8, 2015.

DOI. No. 10.1109/TAES.2015.140351.

Refereeing of this contribution was handled by B.-N. Vo.

Authors' addresses: S. Nannuru, M. Coates, Department of Electrical and Computer Engineering, McGill University, 3480 University Street, Montreal, Quebec H3A 2A7 Canada. E-mail: (santosh.nannuru@mail.mcgill.ca, mark.coates@mcgill.ca).

0018-9251/15/\$26.00 © 2015 IEEE

I. INTRODUCTION

We study the problem of sequential multitarget state estimation from noisy sensor observations. The traditional approach to model the state and observations as random vectors has drawbacks, since it cannot efficiently model the changing multitarget state dimension and observation dimension. To address this issue, Mahler [1] formulated the problem using the random finite set (RFS) framework. In this framework, the multitarget state and the observations are modeled as realizations of random sets. Approximate and computationally feasible multitarget state estimation algorithms have been developed using RFS statistics [1–4].

Most of the research on RFS-based multitarget filtering has made use of a specific type of sensors, which we refer to as standard sensors [5]. The standard-sensor observation model can be characterized as follows: 1) Each target causes either one or no measurement and 2) each measurement is caused by either a single target or clutter. Examples of this category of sensors are range sensors, bearing sensors, radar, and sonar. We are interested in a different but important class of sensors, which we call superpositional sensors [5]. The superpositional-sensor observation model has the following characteristics: 1) Each measurement is affected by multiple targets in an additive fashion—i.e., the contribution to a measurement due to multiple targets is equal to the sum of contributions to that measurement from each of the targets when present alone; 2) each target can potentially affect any number of measurements; and 3) measurements are not independent. Many sensors belong to the category of superpositional sensors. Examples include direction-of-arrival sensors for linear antenna arrays [6], antenna arrays in multiuser detection for wireless communication networks [7], multipath channel modeling in MIMO-OFDM channels [8], acoustic amplitude sensors [9], and radio frequency tomographic tracking systems [10]. In the RFS filter literature under standard-sensor assumptions, both the multitarget state and the observations are modeled as random finite sets. In this work we model the multitarget state as an RFS and the observations as random vectors.

Various filters have been proposed within the RFS framework. These filters differ in the underlying assumption they make about the multitarget state. The probability hypothesis density (PHD) filter [2] assumes the state to be a realization of a Poisson RFS. It has the advantage that a single PHD function can completely characterize the multitarget distribution. The cardinalized probability hypothesis density (CPHD) filter [3] is an improvement over the PHD filter and uses the independent and identically distributed cluster (IIDC) RFS to model the multitarget state. A PHD function and a cardinality distribution are required to characterize the IIDC multitarget distribution. The additional cardinality information improves the performance of the CPHD filter. These filters have been used in various multitarget tracking applications. Some examples include application

of the PHD filter for the problem of passive multistatic radar tracking [11] and the problem of simultaneous localization and mapping [12]. The CPHD filter has been applied for distributed multitarget estimation [13] using the consensus approach.

Both the PHD and CPHD filters use a single density function to represent the multiple single-target states. In contrast, the multi-Bernoulli filter [1, 14] models each target state with a scalar existence probability and a state density function. This allows more accurate state representation and also provides easy track maintenance [1]. A generalization of the multi-Bernoulli filter has been proposed by Vo and Vo [15], called the generalized labeled multi-Bernoulli (GLMB) filter. This provides a closed-form solution to the Bayes recursive filter and can track target labels over time. Since a direct implementation of the GLMB filter can be computationally expensive, efficient approximations have been recently developed [16–18].

From our simulations (see Section VII), we observe that the approximate multi-Bernoulli filter for superpositional sensors makes frequent cardinality errors. We address this issue by using a hybrid multi-Bernoulli CPHD filter in which the new targets are modeled as realizations of the IIDC RFS while the existing targets are modeled using the multi-Bernoulli RFS.

In this paper we provide the derivation of the multi-Bernoulli filter [19] and the hybrid multi-Bernoulli CPHD filter update equations for the superpositional-sensor scenario. A summary of the update equations, without any derivations, was provided in our earlier conference paper [20]. The derivation relies on performing an approximate Bayes update of the PHD of each independent component in the multitarget state. The cardinality distribution of the IIDC component is also updated.

We note that the derivation approach we present for the multi-Bernoulli filters for superpositional sensors is significantly different from that for the multi-Bernoulli filter for standard sensors [1]. The latter uses the probability-generating functional-based formulation of the multitarget Bayes filter [1], which cannot be easily applied for the superpositional observation model. The approximate approach developed in this paper cannot be extended to the standard observation model, because the crucial step of applying Campbell's theorem can only be used when the observation model has a superpositional form.

The remainder of the paper is organized as follows. We summarize the related literature on superpositional sensors and RFS-theory-based filters in Section II. Section III provides the problem formulation and discusses the mathematical formulation of the superpositional-sensor model. A brief review of the concept of RFSs is provided in Section IV. The PHD update mechanism for union of independent random finite sets is also discussed in Section IV. We develop the multi-Bernoulli and hybrid multi-Bernoulli CPHD filter update equations in

Section V. Section VI presents the auxiliary particle-filter implementation of these filters. Section VII compares these filters with the CPHD filter in the context of multitarget tracking using acoustic sensor networks and the radio frequency (RF) tomography measurement model. We provide conclusions in Section VIII.

II. RELATED WORK

Various multitarget tracking filters have recently been proposed for the case of superpositional sensors. Here we provide a brief summary of this literature. A general mathematical description of RFS theory can be found in [1, 21]. The PHD filter for superpositional sensors was derived by Thouin et al. [22].¹ CPHD filter equations for superpositional sensors were first derived in [5] but are computationally intractable. An analytically tractable closed-form Gaussian-mixture-based implementation of the CPHD filter for superpositional sensors was derived by Hauschildt [26]. Building on the derivation approach proposed by Thouin et al. [22], Mahler and El-Fallah derived a computationally tractable CPHD filter for superpositional sensors [24]. An auxiliary particle-filter implementation of the PHD and CPHD filters for superpositional sensors was presented in [25]. The PHD and CPHD filters for superpositional sensors are extensively discussed in [21].

The multi-Bernoulli filter was adapted for estimation and detection of multiple objects from image observations in track-before-detect applications [27] under the assumption that the likelihood has a separable form. This assumption is valid when the objects are nonoverlapping. Hoseinnezhad et al. [28] used this filter for tracking multiple targets in background-subtracted image sequences. The particle-based implementation of the multi-Bernoulli filter has been discussed in [14].

We proposed the multi-Bernoulli filter for superpositional sensors in [19]. We presented a particle-filter implementation of this filter in [29]. This implementation is similar to the multiple particle filter proposed in [30] in the sense that both use one particle filter per target. The multiple particle filter assumes the number of targets to be fixed and known, but the multi-Bernoulli filter automatically tracks the changing number of targets. The update step in the multiple particle filter propagates the marginal posterior, whereas the update step in the multi-Bernoulli filter propagates the PHD.

Some recent research has focused on labeled random finite sets and the corresponding GLMB filter and its approximations. These can be applied to the superpositional-sensor model. In [31], Papi and Kim proposed a particle-based multitarget tracking algorithm for superpositional measurements. They used the approximate CPHD filter [25] update equations to design proposal distributions for propagating labeled random

¹ An error in the main update equation of this filter was corrected in an erratum [23]; the correct equations were also presented in [24, 25].

finite sets over time. An approximation mechanism is developed in [32] for multitarget tracking using labeled random finite sets; this is applicable to any generic measurement model, including the superpositional-sensor model. Labeled RFS-based tracking has also been applied for the case of merged measurements [33], where groups of closely spaced targets can generate a single merged measurement.

All of these filters use a single kind of random finite set to model the multitarget state. We can benefit by modeling the multitarget state as a union of different kinds of random finite sets. Some of the hybrid approaches proposed in the literature for the case of standard sensors are discussed next. A hybrid of the multi-Bernoulli filter and the PHD filter was developed by Williams [34] for multitarget tracking applications, using a Poisson RFS to model new targets and targets with a low probability of existence. This results in fast track initiation and use of fewer Bernoulli components. Pollard et al. [35] used a hybrid combination of the multiple hypothesis tracking (MHT) filter and the Gaussian-mixture CPHD filter for multitarget tracking. The Gaussian-mixture CPHD filter provides a robust cardinality estimate of the multitarget state, which is complemented by accurate state estimates from the MHT filter. A combination of the MHT and PHD filters was utilized by Panta et al. to obtain track-valued estimates [36]. They used the PHD filter as a clutter filter by using its output to gate the input for the MHT filter. To the best of our knowledge, no hybrid filter has been developed previously for the case of superpositional sensors.

III. PROBLEM FORMULATION AND SENSOR MODEL

In this paper we study superpositional sensors in the context of the multitarget tracking problem. The multitarget state is the set $X_k = \{\mathbf{x}_{k,1}, \mathbf{x}_{k,2}, \dots, \mathbf{x}_{k,n_k}\}$, where $\mathbf{x}_{k,i}$, $i = 1, 2, \dots, n_k$ are the single-target state vectors of the $n_k \geq 0$ targets present at time step k . The single-target state dimension is n_x , so $\mathbf{x}_{k,i} \in R^{n_x} \forall i$. The targets move independently and their motion is governed by the Markovian transition kernel $t_{k|k-1}(\mathbf{x}_{k,i}|\mathbf{x}_{k-1,i}, \mathbf{u}_k)$, where \mathbf{u}_k is the Gaussian noise vector. This state information is hidden, but we have access to the observation vector $\mathbf{z}_k \in R^{n_z}$ at time step k . The observations are related to the multitarget state through the likelihood function $h_{\mathbf{z}_k}(X_k)$. Let $Z^{[k]} = [\mathbf{z}_1, \mathbf{z}_2, \dots, \mathbf{z}_k]$ be the collection of all the observation vectors up to time k . The multitarget tracking problem is to estimate the posterior multitarget state density $p(X_k|Z^{[k]})$ at each time step k . For a known model of the multitarget state, we estimate the sufficient statistics of the posterior multitarget state density.

A. Superpositional-Sensor Model

The likelihood function under the superpositional model assumption has the following form:

$$h_{\mathbf{z}_k}(X_k) = h_{\mathbf{z}_k}(\zeta(X_k)) \quad (1)$$

$$= h_{\mathbf{z}_k}\left(\sum_{\mathbf{x} \in X_k} g(\mathbf{x})\right), \quad (2)$$

where $h_{\mathbf{z}_k}$ is the real-valued likelihood function and g and ζ are (potentially nonlinear) functions mapping to vectors of reals. When the sensor observation noise is Gaussian with zero mean and covariance matrix Σ_z , the likelihood takes the form

$$h_{\mathbf{z}_k}(X_k) = \mathcal{N}_{\Sigma_z}(\mathbf{z}_k - \zeta(X_k)), \quad (3)$$

where $\mathcal{N}_{\Sigma}(\mathbf{z})$ denotes the Gaussian density function with zero mean and covariance matrix Σ evaluated at \mathbf{z} .

IV. RANDOM FINITE SETS

Random sets are an extension of the concept of random variables and random vectors. While random vectors are of a predefined dimension and have an ordering of their elements, random sets can have uncertainty in the set dimension, and there is no preferred ordering of the elements of the set.

We can associate a probability density function $f(W)$ with a random finite set Ξ which integrates to 1. Since it is a function defined over sets, its integral is defined as

$$\int f(W) \delta W = f(\emptyset) + \sum_{n=1}^{\infty} \frac{1}{n!} \int f(W_n) dW_n = 1, \quad (4)$$

where \emptyset is the empty set. The notation δW denotes set integration, and δW_n denotes standard integration. We have used the abbreviated notation $W_n = \{\mathbf{w}_1, \dots, \mathbf{w}_n\}$ and $dW_n = d\mathbf{w}_1 \dots d\mathbf{w}_n$ for brevity. The associated cardinality distribution of the RFS is given by

$$\text{Prob}(|\Xi| = n) = \pi(n) = \frac{1}{n!} \int_{|W|=n} f(W) \delta W. \quad (5)$$

Since the addition operation is not naturally defined on sets, defining the expectation of an RFS in the traditional manner is not possible. An important and useful statistic of the RFS which can be defined using a modified definition of the first moment [1] is the probability hypothesis density. The PHD of an RFS with a probability density $f(W)$ is

$$D(\mathbf{x}) = \int f(\{\mathbf{x}\} \cup W) \delta W. \quad (6)$$

Similarly, the second factorial moment is defined as

$$D(\{\mathbf{x}_1, \mathbf{x}_2\}) = \int f(\{\mathbf{x}_1, \mathbf{x}_2\} \cup W) \delta W. \quad (7)$$

A. IIDC RFS

An IIDC RFS is specified using an arbitrary cardinality distribution $\pi^c(n)$ and a density function $q_c(\mathbf{x})$. The PHD of the IIDC RFS is

$$D^c(\mathbf{x}) = \int f(\{\mathbf{x}\} \cup W) \delta W = \mu_c q_c(\mathbf{x}), \quad (8)$$

$$\mu_c = \sum_{n=0}^{\infty} n \pi^c(n), \quad (9)$$

where μ_c is the mean cardinality. Its second factorial moment can be calculated [24] to be

$$D^c(\{\mathbf{x}_1, \mathbf{x}_2\}) = a q_c(\mathbf{x}_1) q_c(\mathbf{x}_2), \quad (10)$$

$$a = \sum_{n=0}^{\infty} n(n-1) \pi^c(n). \quad (11)$$

B. Multi-Bernoulli RFS

To understand the multi-Bernoulli RFS, let us first consider the Bernoulli RFS. A Bernoulli RFS can be either an empty set with probability $1 - r$ or a singleton set $\{\mathbf{x}\}$ with probability r ; the singleton element \mathbf{x} , when present, is drawn from the distribution function $q(\mathbf{x})$. The PHD function of the Bernoulli RFS is given by

$$D^b(\mathbf{x}) = \int f(\{\mathbf{x}\} \cup W) \delta W = r q(\mathbf{x}). \quad (12)$$

The Bernoulli RFS can be used to model a single target. To represent multiple targets, its extension the multi-Bernoulli RFS can be used [1]. A multi-Bernoulli RFS Ξ is defined as the union of N independent Bernoulli RFS components, $\Xi = \Xi_1 \cup \Xi_2 \cup \dots \cup \Xi_N$, where each Ξ_i is a Bernoulli RFS with parameters given by $\{r_i, q_i(\mathbf{x})\}_{i=1}^N$. The PHD of the multi-Bernoulli RFS [1, chapter 16, example 91] is

$$D^{\text{mb}}(\mathbf{x}) = \sum_{i=1}^N r_i q_i(\mathbf{x}). \quad (13)$$

The second factorial moment of the multi-Bernoulli RFS [19] is

$$D^{\text{mb}}(\{\mathbf{x}_1, \mathbf{x}_2\}) = \sum_{i=1}^N \sum_{j=1, j \neq i}^N r_i r_j q_i(\mathbf{x}_1) q_j(\mathbf{x}_2) \quad (14)$$

$$= D^{\text{mb}}(\mathbf{x}_1) D^{\text{mb}}(\mathbf{x}_2) - \sum_{i=1}^N r_i^2 q_i(\mathbf{x}_1) q_i(\mathbf{x}_2). \quad (15)$$

C. Union of Statistically Independent Random Finite Sets

Consider an RFS Ξ which is the union of multiple (M) statistically independent random finite sets $\Xi^1, \Xi^2, \dots, \Xi^M$, given by $\Xi = \Xi^1 \cup \Xi^2 \cup \Xi^3 \cup \dots \cup \Xi^M$. The random finite sets $\Xi^1, \Xi^2, \dots, \Xi^M$ can be sets of any kind. For example, in this paper we consider them to be a Bernoulli RFS, a multi-Bernoulli RFS, or an IIDC RFS. We refer to these individual constituent random finite sets of Ξ as components of Ξ . We consider the union of statistically independent random finite sets, as this allows us to approximately propagate the PHD function of the individual components over time.

Let the PHD function for each of the RFS components be denoted respectively by $D^1(\mathbf{x}), D^2(\mathbf{x}), D^3(\mathbf{x}), \dots$,

$D^M(\mathbf{x})$. Let the PHD of the RFS Ξ be denoted $D(\mathbf{x})$; then

$$D(\mathbf{x}) = D^1(\mathbf{x}) + D^2(\mathbf{x}) + D^3(\mathbf{x}) + \dots + D^M(\mathbf{x}). \quad (16)$$

This result can be easily proved using the properties of the probability-generating functional and the basic rules for functional derivatives [1].

Let $f^1(W), f^2(W), \dots, f^M(W)$ be, respectively, the multitarget probability densities of the random finite sets $\Xi^1, \Xi^2, \dots, \Xi^M$. Let $f(W)$ be the multitarget probability density of the random finite set Ξ given by the union $\Xi = \Xi^1 \cup \Xi^2 \cup \Xi^3 \cup \dots \cup \Xi^M$. Then we have the following convolution relation between the densities [1, section 11.5.3]:

$$f(W) = \sum_{Y^1 \uplus Y^2 \uplus \dots \uplus Y^M = W} f^1(Y^1) f^2(Y^2) \dots f^M(Y^M), \quad (17)$$

where the summation is over all mutually disjoint subsets Y^1, Y^2, \dots, Y^M of W such that $Y^1 \cup Y^2 \cup \dots \cup Y^M = W$. The notation \uplus is used to emphasize that the union is over mutually disjoint sets.

D. PHD Update for the Union of Statistically Independent Random Finite Sets

In this section we analyze the PHD update step when the multitarget state can be expressed as union of multiple statistically independent random finite sets. Let the predicted multitarget state at time $k + 1$ be modeled as a random finite set $\Xi_{k+1|k}$ with density $f_{k+1|k}(W)$ and PHD $D_{k+1|k}(\mathbf{x})$. Further, assume that $\Xi_{k+1|k}$ is the union of statistically independent random finite sets $\Xi_{k+1|k}^1, \Xi_{k+1|k}^2, \dots, \Xi_{k+1|k}^M$ with, respectively, densities $f_{k+1|k}^1(Y), f_{k+1|k}^2(Y), \dots, f_{k+1|k}^M(Y)$ and PHDs $D_{k+1|k}^1(\mathbf{x}), D_{k+1|k}^2(\mathbf{x}), \dots, D_{k+1|k}^M(\mathbf{x})$. Then from (16) and (17), we have

$$f_{k+1|k}(W) = \sum_{Y^1 \uplus \dots \uplus Y^M = W} \prod_{A=1}^M f_{k+1|k}^A(Y^A), \quad (18)$$

where the summation is over all mutually disjoint subsets Y^1, Y^2, \dots, Y^M of W such that $Y^1 \cup Y^2 \cup \dots \cup Y^M = W$ and

$$D_{k+1|k}(\mathbf{x}) = D_{k+1|k}^1(\mathbf{x}) + D_{k+1|k}^2(\mathbf{x}) + \dots + D_{k+1|k}^M(\mathbf{x}). \quad (19)$$

Let $f_{k+1}(W)$ and $D_{k+1}(\mathbf{x})$ be the density and PHD of the posterior multitarget state. Then we have

$$D_{k+1}(\mathbf{x}) = \int f_{k+1}(\{\mathbf{x}\} \cup W) \delta W. \quad (20)$$

Applying Bayes's rule, we get

$$D_{k+1}(\mathbf{x}) = \frac{\int h_{\mathbf{z}_{k+1}}(\{\mathbf{x}\} \cup W) f_{k+1|k}(\{\mathbf{x}\} \cup W) \delta W}{f_{k+1}(\mathbf{z}_{k+1}|Z^{[k]})}. \quad (21)$$

From (18) we have

$$\begin{aligned} f_{k+1|k}(\{\mathbf{x}\} \cup W) &= \sum_{A=1}^M \sum_{Y^1 \uplus \dots \uplus Y^M = W} f_{k+1|k}^A(\{\mathbf{x}\} \cup Y^A) \prod_{j \neq A} f_{k+1|k}^j(Y^j) \end{aligned} \quad (22)$$

$$\begin{aligned} &= \sum_{A=1}^M D_{k+1|k}^A(\mathbf{x}) \times \sum_{Y^1 \uplus \dots \uplus Y^M = W} \frac{f_{k+1|k}^A(\{\mathbf{x}\} \cup Y^A)}{D_{k+1|k}^A(\mathbf{x})} \\ &\quad \times \prod_{j \neq A} f_{k+1|k}^j(Y^j). \end{aligned} \quad (23)$$

We can simplify this as

$$\begin{aligned} f_{k+1|k}(\{\mathbf{x}\} \cup W) &= \sum_{A=1}^M D_{k+1|k}^A(\mathbf{x}) \sum_{Y^1 \uplus \dots \uplus Y^M = W} f_{k+1|k}^{A_x}(Y^A) \\ &\quad \times \prod_{j \neq A} f_{k+1|k}^j(Y^j), \end{aligned} \quad (24)$$

where $f_{k+1|k}^{A_x}(Y)$ is defined as

$$f_{k+1|k}^{A_x}(Y) = \frac{f_{k+1|k}^A(\{\mathbf{x}\} \cup Y)}{D_{k+1|k}^A(\mathbf{x})} \quad (25)$$

for $A = 1, 2, \dots, M$. These are valid multitarget densities which integrate to 1 from the definition of PHD in (6).

Now denote

$$f_{k+1|k}^{A_x^*}(W) = \sum_{Y^1 \uplus \dots \uplus Y^M = W} f_{k+1|k}^{A_x}(Y^A) \prod_{j \neq A} f_{k+1|k}^j(Y^j) \quad (26)$$

for $A = 1, 2, \dots, M$, which are valid multitarget densities.

We note that the density $f_{k+1|k}^{A_x^*}(W)$ is obtained by replacing $f_{k+1|k}^A(Y^A)$ with $f_{k+1|k}^{A_x}(Y^A)$ in (18). Using this notation we can write

$$f_{k+1|k}(\{\mathbf{x}\} \cup W) = \sum_{A=1}^M D_{k+1|k}^A(\mathbf{x}) f_{k+1|k}^{A_x^*}(W). \quad (27)$$

Substituting (27) in (21), we have

$$D_{k+1}(\mathbf{x}) = \sum_{A=1}^M D_{k+1|k}^A(\mathbf{x}) \frac{\int h_{\mathbf{z}_{k+1}}(\{\mathbf{x}\} \cup W) f_{k+1|k}^{A_x^*}(W) \delta W}{f_{k+1}(\mathbf{z}_{k+1}|Z^{[k]})}. \quad (28)$$

Now define

$$D_{k+1}^A(\mathbf{x}) = D_{k+1|k}^A(\mathbf{x}) \frac{\int h_{\mathbf{z}_{k+1}}(\{\mathbf{x}\} \cup W) f_{k+1|k}^{A_x^*}(W) \delta W}{f_{k+1}(\mathbf{z}_{k+1}|Z^{[k]})} \quad (29)$$

for $A = 1, 2, \dots, M$.

We now assume that the posterior multitarget state at time $k + 1$ is a union of statistically independent

random finite sets $\Xi_{k+1}^1, \Xi_{k+1}^2, \dots, \Xi_{k+1}^M$. Let $D_{k+1}^1(\mathbf{x}), \dots, D_{k+1}^M(\mathbf{x})$ be their PHD functions. Then from (19), (28), and (29) we have

$$\sum_{A=1}^M D_{k+1}^A(\mathbf{x}) = \sum_{A=1}^M D_{k+1}^A(\mathbf{x}). \quad (30)$$

To derive an update mechanism for propagating the PHD over time, we make the following separability assumption on the PHD of the different components:

$$D_{k+1}^A(\mathbf{x}) \approx \mathcal{D}_{k+1}^A(\mathbf{x}) \quad (31)$$

for all $A = 1, 2, \dots, M$.

This one-to-one matching is an approximation and is based on the assumption that the posterior multitarget state is also a union of independent random finite sets and that for each component in the predicted multitarget state we have a corresponding component of the same type in the posterior multitarget state. This approximation is justified under the assumption that the supports of the PHD functions of the two components are well separated. This is a good approximation if each component represents a single target or a group of targets which are well separated in the state space.

This approximation allows us to relate the posterior and predicted PHD functions, using (29) and (31), as follows:

$$D_{k+1}^A(\mathbf{x}) \approx \mathcal{D}_{k+1|k}^A(\mathbf{x}) \frac{\int h_{\mathbf{z}_{k+1}}(\{\mathbf{x}\} \cup W) f_{k+1|k}^{A_x^*}(W) \delta W}{f_{k+1}(\mathbf{z}_{k+1}|Z^{[k]})}. \quad (33)$$

In general we can update the PHD of each individual RFS component of the multitarget state using this approximation. We apply this PHD update mechanism for two specific cases: when the multitarget state is modeled as a union of independent Bernoulli RFS components, leading to the multi-Bernoulli filter, and when it is modeled as a union of independent multi-Bernoulli RFS and IIDC RFS components, leading to the hybrid multi-Bernoulli CPHD filter.

V. MULTI-BERNOULLI FILTERS FOR THE SUPERPOSITIONAL-SENSOR MODEL

In this section we approximate the PHD update scheme proposed in Section IV-D for the case of the superpositional-sensor model under the assumption of Gaussian sensor noise. This approximation leads to a computationally tractable update equation for the PHD of individual components. This result is applied in later subsections for deriving the update equations of the multi-Bernoulli filter and the hybrid multi-Bernoulli CPHD filter.

A. Approximate PHD Update for the Superpositional-Sensor Model with Gaussian Sensor Noise

From (29) we have

$$\begin{aligned} \mathcal{D}_{k+1}^A(\mathbf{x}) &= D_{k+1|k}^A(\mathbf{x}) \frac{\int h_{\mathbf{z}_{k+1}}(\{\mathbf{x}\} \cup W) f_{k+1|k}^{A*}(W) \delta W}{f_{k+1}(\mathbf{z}_{k+1}|Z^{[k]})} \end{aligned} \quad (34)$$

$$= D_{k+1|k}^A(\mathbf{x}) \frac{\int h_{\mathbf{z}_{k+1}}(\{\mathbf{x}\} \cup W) f_{k+1|k}^{A*}(W) \delta W}{\int h_{\mathbf{z}_{k+1}}(W) f_{k+1|k}(W) \delta W}. \quad (35)$$

Using the assumption of Gaussian sensor noise and the superpositional likelihood model from (2) and (3), we have

$$\begin{aligned} \mathcal{D}_{k+1}^A(\mathbf{x}) &= D_{k+1|k}^A(\mathbf{x}) \\ &\times \frac{\int \mathcal{N}_{\Sigma_z}(\mathbf{z}_{k+1} - g(\mathbf{x}) - \zeta(W)) f_{k+1|k}^{A*}(W) \delta W}{\int \mathcal{N}_{\Sigma_z}(\mathbf{z}_{k+1} - \zeta(W)) f_{k+1|k}(W) \delta W}. \end{aligned} \quad (36)$$

We apply the transformation $\mathbf{y}^* = \zeta(W)$ in the numerator and $\mathbf{y} = \zeta(W)$ in the denominator. Using the formula for change of variables for set integrals (24), we have

$$\begin{aligned} \mathcal{D}_{k+1}^A(\mathbf{x}) &= D_{k+1|k}^A(\mathbf{x}) \\ &\times \frac{\int \mathcal{N}_{\Sigma_z}(\mathbf{z}_{k+1} - g(\mathbf{x}) - \mathbf{y}^*) Q_{k+1|k}^{A*}(\mathbf{y}^*) d\mathbf{y}^*}{\int \mathcal{N}_{\Sigma_z}(\mathbf{z}_{k+1} - \mathbf{y}) Q_{k+1|k}(\mathbf{y}) d\mathbf{y}}, \end{aligned} \quad (37)$$

where $Q_{k+1|k}(\mathbf{y})$ and $Q_{k+1|k}^{A*}(\mathbf{y}^*)$ are the probability distributions of the random vectors \mathbf{y} and \mathbf{y}^* , respectively. Using a Gaussian approximation for these densities,

$Q_{k+1|k}(\mathbf{y}) \approx \mathcal{N}_{\Sigma_{k+1}}(\mathbf{y} - \mu_{k+1})$ and $Q_{k+1|k}^{A*}(\mathbf{y}^*) \approx \mathcal{N}_{\Sigma_{k+1}^{A*}}(\mathbf{y}^* - \mu_{k+1}^{A*})$, we have

$$\begin{aligned} \mathcal{D}_{k+1}^A(\mathbf{x}) &\approx D_{k+1|k}^A(\mathbf{x}) \\ &\times \frac{\int \mathcal{N}_{\Sigma_z}(\mathbf{z}_{k+1} - g(\mathbf{x}) - \mathbf{y}^*) \mathcal{N}_{\Sigma_{k+1}^{A*}}(\mathbf{y}^* - \mu_{k+1}^{A*}) d\mathbf{y}^*}{\int \mathcal{N}_{\Sigma_z}(\mathbf{z}_{k+1} - \mathbf{y}) \mathcal{N}_{\Sigma_{k+1}}(\mathbf{y} - \mu_{k+1}) d\mathbf{y}}. \end{aligned} \quad (38)$$

This equation can be simplified using the following result: $\int \mathcal{N}_{\Sigma_1}(a - \mathbf{y}) \times \mathcal{N}_{\Sigma_2}(\mathbf{y} - b) d\mathbf{y} = \mathcal{N}_{\Sigma_1 + \Sigma_2}(a - b)$. Combining the approximations in (33) and (38), the approximate PHD update equation for the superpositional-sensor model with Gaussian sensor noise is

$$D_{k+1}^A(\mathbf{x}) \approx D_{k+1|k}^A(\mathbf{x}) \frac{\mathcal{N}_{\Sigma_z + \Sigma_{k+1}^{A*}}(\mathbf{z}_{k+1} - g(\mathbf{x}) - \mu_{k+1}^{A*})}{\mathcal{N}_{\Sigma_z + \Sigma_{k+1}}(\mathbf{z}_{k+1} - \mu_{k+1})}, \quad (39)$$

where μ_{k+1} and Σ_{k+1} are the mean and covariance matrix of the distribution $Q_{k+1|k}(\mathbf{y})$, and μ_{k+1}^{A*} and Σ_{k+1}^{A*} are the mean and covariance matrix of the distribution $Q_{k+1|k}^{A*}(\mathbf{y}^*)$. These mean and covariance-matrix parameters can be found using the quadratic version of Campbell's

theorem [24, 25]. Through modeling of the unknown multitarget state as a union of independent random finite sets, different tracking filters can be derived whose update equations are special cases of (39).

The approximations $Q_{k+1|k}(\mathbf{y}) \approx \mathcal{N}_{\Sigma_{k+1}}(\mathbf{y} - \mu_{k+1})$ and $Q_{k+1|k}^{A*}(\mathbf{y}^*) \approx \mathcal{N}_{\Sigma_{k+1}^{A*}}(\mathbf{y}^* - \mu_{k+1}^{A*})$ have been introduced in order to analytically evaluate the integrals in (37). Without this approximation, the update equation would involve integrals which have to be numerically evaluated and would make the filter implementation computationally demanding. We have performed a brief numerical analysis of the errors introduced in the integral because of this approximation, and the detailed results are available in [37]. To summarize, we observe that as the average number of targets represented by the underlying random finite sets is increased, the error between the original and the approximated integral decreases significantly. For different kinds of random finite sets, the accuracy of the approximation varies. The approximation is most accurate for an IIDC RFS, followed by a union of multi-Bernoulli and IIDC RFS; it is least accurate for a multi-Bernoulli RFS.

B. Multi-Bernoulli Filter

The multi-Bernoulli filter models the multitarget state as the union of multiple independent Bernoulli random finite sets. The scalar existence probability and the single-target state density for each Bernoulli component are propagated over time. The propagation is done in two stages: prediction and update. The model for target dynamics accounts for the survival of existing targets from the previous time step to the current time step and for the birth of new targets. The single-target motion model is used for propagation of surviving targets in the prediction step. Target birth is modeled as a multi-Bernoulli RFS. We do not consider target spawning in this paper. The most recent observation, along with the likelihood model, is used in the update step to propagate the Bernoulli parameters.

1) *Prediction Step:* The multi-Bernoulli prediction equations are derived in [1, 38]. Since the superpositional observation model does not play a role in the prediction step, the multi-Bernoulli prediction equations remain the same. We briefly review these equations in this section.

Let the existence probability and state density parameters of the N_k targets at time k be $\{r_{k,i}, q_{k,i}(\mathbf{x})\}_{i=1}^{N_k}$. At time $k+1$, let there be $N_{k+1|k}$ predicted targets with parameters $r_i = r_{k+1|k,i}$ and $q_i(\mathbf{x}) = q_{k+1|k,i}(\mathbf{x})$. Additionally, the predicted multi-Bernoulli RFS parameters can be expressed as

$$\{r_i, q_i(\mathbf{x})\}_{i=1}^{N_{k+1|k}} = \{r_i^P, q_i^P(\mathbf{x})\}_{i=1}^{N_k} \cup \{r_i^B, q_i^B(\mathbf{x})\}_{i=N_k+1}^{N_{k+1|k}}, \quad (40)$$

where $\{r_i^P, q_i^P(\mathbf{x})\}_{i=1}^{N_k}$ are the parameters of targets propagated from the previous time step and $\{r_i^B, q_i^B(\mathbf{x})\}_{i=N_k+1}^{N_{k+1|k}}$ are the parameters of newly born targets.

The relation between the predicted target parameters at time $k + 1$ and the posterior target parameters at time k is

$$r_i^P = r_{k,i} \langle q_{k,i}, p_s \rangle \quad (41)$$

and

$$q_i^P(\mathbf{x}) = \frac{\langle t_{k+1|k}(\mathbf{x}|\cdot), q_{k,i} p_s \rangle}{\langle q_{k,i}, p_s \rangle}, \quad (42)$$

where $p_s(\mathbf{x})$ is the target survival probability, $t_{k+1|k}(\mathbf{x}|\cdot)$ is the Markov transition kernel, and $\langle a, b \rangle$ is the scalar product defined as $\langle a, b \rangle = \int a(\mathbf{x})b(\mathbf{x})d\mathbf{x}$. Since the parameters $\{r_i^B, q_i^B(\mathbf{x})\}_{i=N_k+1}^{N_{k+1}}$ are used to model the new targets arriving at time $k + 1$, they are initialized using the target birth model.

2) *Update Step:* We assume that the posterior multitarget density also has the multi-Bernoulli form. For the case of superpositional sensors, the measurements do not provide any direct information about the number of targets. Hence, no new Bernoulli components are added in the update step and $N_{k+1} = N_{k+1|k}$. Since the PHD of all the individual Bernoulli components taken together can completely specify the posterior multi-Bernoulli density, the update step consists of updating the PHD for each of the $i = 1, 2, \dots, N_{k+1}$ Bernoulli components. Let $\{r'_i, q'_i(\mathbf{x})\}_{i=1}^{N_{k+1}}$ denote the parameter set of the posterior multi-Bernoulli density at time $k + 1$. Combining the results from [12] and [39], the approximate PHD update is given by

$$r'_i q'_i(\mathbf{x}) \approx r_i q_i(\mathbf{x}) \frac{\mathcal{N}_{\Sigma_{\mathbf{z}} + \Sigma_{k+1}}(\mathbf{z}_{k+1} - g(\mathbf{x}) - \mu_{k+1}^{\bar{i}})}{\mathcal{N}_{\Sigma_{\mathbf{z}} + \Sigma_{k+1}}(\mathbf{z}_{k+1} - \mu_{k+1})} \quad (43)$$

where

$$\mu_{k+1} = \sum_{i=1}^{N_{k+1|k}} r_i s_i, \quad (44)$$

$$\Sigma_{k+1} = \sum_{i=1}^{N_{k+1|k}} (r_i v_i - r_i^2 s_i s_i^T), \quad (45)$$

$$\mu_{k+1}^{\bar{i}} = \mu_{k+1}^{A_x^*} = \mu_{k+1} - r_i s_i, \quad (46)$$

$$\Sigma_{k+1}^{\bar{i}} = \Sigma_{k+1}^{A_x^*} = \Sigma_{k+1} - (r_i v_i - r_i^2 s_i s_i^T), \quad (47)$$

and

$$s_i = \langle q_i, g \rangle, \quad v_i = \langle q_i, g g^T \rangle. \quad (48)$$

The expressions for these parameters are derived in Appendix A. From (44)–(48) we see that the quantities $\mu_{k+1}^{A_x^*}$ and $\Sigma_{k+1}^{A_x^*}$ do not depend on \mathbf{x} when $\Xi_{k+1|k}^A$ is a Bernoulli RFS.

C. Hybrid Multi-Bernoulli CPHD Filter

The multi-Bernoulli RFS modeling of the multitarget state allows us to model each of the targets individually

and update its state information. Although this can be seen as an improvement over the IIDC RFS modeling of the multitarget state, which utilizes only one state density function to model all of the targets, estimating the number of targets using the multi-Bernoulli RFS model is inaccurate in practice. Also, since the number of targets is changing over time, we need to add multiple Bernoulli components at each time step to account for target births. Processing a large number of Bernoulli components at each time step is not computationally efficient. To address these drawbacks, we propose to use a hybrid approach, where the existing targets are modeled using a multi-Bernoulli RFS and the newborn targets are modeled using the IIDC RFS.

The hybrid multi-Bernoulli CPHD filter uses the following modeling scheme. The final posterior distribution from the previous time step is modeled as a multi-Bernoulli RFS. In the prediction step, the multi-Bernoulli component is propagated following the motion model of surviving targets, whereas to account for newborn targets an IIDC RFS component is initialized. The IIDC component is independent of the multi-Bernoulli component. Thus the predicted distribution corresponds to the union of an IIDC random finite set and a multi-Bernoulli random finite set, and these sets are independent. The union is completely represented by the PHD of the Bernoulli components, the PHD of the IIDC component, and the cardinality distribution of the IIDC component. The update step propagates all of these quantities using Bayes's rule. Hence the obtained posterior is the union of an IIDC component and a multi-Bernoulli component. Since individual targets are better represented using Bernoulli random finite sets, the updated IIDC component is then approximated using multiple Bernoulli components. Thus the final posterior distribution is modeled using a multi-Bernoulli random finite set.

1) *Prediction Step:* Let the parameters of the posterior Bernoulli components at time step k be denoted $\{r_{k,i}, q_{k,i}(\mathbf{x})\}_{i=1}^{N_k}$ as before. The Bernoulli parameters at the end of the prediction step are $\{r_i, q_i(\mathbf{x})\}_{i=1}^{N_k}$ and are given by (41) and (42). Let $\pi_{k+1|k}^c(n)$ and $q_c(\mathbf{x}) = q_{c,k+1|k}(\mathbf{x})$ be the predicted cardinality distribution and the predicted density function of the IIDC component at time $k + 1$. Their exact forms depend on the specific target birth model used. Let μ_c denote the expected cardinality of the predicted IIDC RFS component. Note that no new Bernoulli components are added in the prediction step to account for the birth of new targets.

2) *Update Step:* The update step consists of updating the PHD for each of the Bernoulli components, the PHD of the IIDC component, and the cardinality distribution of the IIDC component. Let the parameters of the posterior multi-Bernoulli and IIDC random finite sets be denoted by $\{r'_i, q'_i(\mathbf{x})\}_{i=1}^{N_k}$ and $\{q'_c(\mathbf{x}), \pi_{k+1}^c(n)\}$, respectively.

From (12) and (39), the PHD update of the i th Bernoulli component is given by

$$r'_i q'_i(\mathbf{x}) \approx r_i q_i(\mathbf{x}) \frac{\mathcal{N}_{\Sigma_z + \Sigma_{k+1}^{\bar{i}}}(\mathbf{z}_{k+1} - g(\mathbf{x}) - \mu_{k+1}^{\bar{i}})}{\mathcal{N}_{\Sigma_z + \Sigma_{k+1}}(\mathbf{z}_{k+1} - \mu_{k+1})}, \quad (49)$$

where

$$\mu_{k+1} = \sum_{i=1}^{N_k} r_i s_i + \mu_c s_c, \quad (50)$$

$$\Sigma_{k+1} = \sum_{i=1}^{N_k} (r_i v_i - r_i^2 s_i s_i^T) + \mu_c v_c - (\mu_c^2 - a) s_c s_c^T, \quad (51)$$

$$\mu_{k+1}^{\bar{i}} = \mu_{k+1}^{A_x^*} = \mu_{k+1} - r_i s_i, \quad (52)$$

$$\Sigma_{k+1}^{\bar{i}} = \Sigma_{k+1}^{A_x^*} = \Sigma_{k+1} - (r_i v_i - r_i^2 s_i s_i^T), \quad (53)$$

$$s_i = \langle q_i, g \rangle, \quad v_i = \langle q_i, g g^T \rangle, \quad s_c = \langle q_c, g \rangle, \quad v_c = \langle q_c, g g^T \rangle, \quad (54)$$

and

$$a = \sum_{n=0}^{\infty} n(n-1) \pi_{k+1|k}^c(n). \quad (55)$$

The equations for the parameters μ_{k+1} , Σ_{k+1} , $\mu_{k+1}^{\bar{i}}$, and $\Sigma_{k+1}^{\bar{i}}$ are derived in Appendix A.

Using (8) and (39), the PHD update for the IIDC RFS component is

$$\mu'_c q'_c(\mathbf{x}) \approx \mu_c q_c(\mathbf{x}) \frac{\mathcal{N}_{\Sigma_z + \Sigma_{k+1}^{\bar{c}}}(\mathbf{z}_{k+1} - g(\mathbf{x}) - \mu_{k+1}^{\bar{c}})}{\mathcal{N}_{\Sigma_z + \Sigma_{k+1}}(\mathbf{z}_{k+1} - \mu_{k+1})}, \quad (56)$$

where

$$\mu_{k+1}^{\bar{c}} = \mu_{k+1}^{A_x^*} = \sum_{j=1}^{N_k} r_j s_j + \frac{a}{\mu_c} s_c, \quad (57)$$

$$\Sigma_{k+1}^{\bar{c}} = \Sigma_{k+1}^{A_x^*} \quad (58)$$

$$= \sum_{j=1}^{N_k} (r_j v_j - r_j^2 s_j s_j^T) + \frac{a}{\mu_c} v_c - \left(\frac{a^2}{\mu_c^2} - \frac{b}{\mu_c} \right) s_c s_c^T, \quad (59)$$

and

$$b = \sum_{n=0}^{\infty} n(n-1)(n-2) \pi_{k+1|k}^c(n). \quad (60)$$

The parameters μ_{k+1} and Σ_{k+1} are as given in (50) and (51), respectively. The derivation of the parameters $\mu_{k+1}^{\bar{c}}$ and $\Sigma_{k+1}^{\bar{c}}$ is provided in Appendix A. From (57)–(60) we see that the quantities $\mu_{k+1}^{A_x^*} = \mu_{k+1}^{\bar{c}}$ and $\Sigma_{k+1}^{A_x^*} = \Sigma_{k+1}^{\bar{c}}$ do not depend on \mathbf{x} when $\Xi_{k+1|k}^{A_x^*}$ is an IIDC RFS.

The main advantage of the IIDC component in the hybrid filter is that we can make use of the accurate cardinality estimation of the CPHD filter. The update equation for the cardinality distribution of the IIDC RFS component is

$$\pi_{k+1}^c(n) \approx \pi_{k+1|k}^c(n) \frac{\mathcal{N}_{\Sigma_z + \Sigma_{k+1}^{c,n}}(\mathbf{z}_{k+1} - \mu_{k+1}^{c,n})}{\mathcal{N}_{\Sigma_z + \Sigma_{k+1}}(\mathbf{z}_{k+1} - \mu_{k+1})}, \quad (61)$$

where

$$\mu_{k+1}^{c,n} = \sum_{i=1}^{N_{k+1|k}} r_i s_i + n s_c \quad (62)$$

and

$$\Sigma_{k+1}^{c,n} = \sum_{i=1}^{N_{k+1|k}} (r_i v_i - r_i^2 s_i s_i^T) + n(v_c - s_c s_c^T). \quad (63)$$

The parameters μ_{k+1} and Σ_{k+1} are as given in (50) and (51), respectively. Appendix B derives the cardinality update equation. Note that the multi-Bernoulli filter can be treated as a special case of the hybrid multi-Bernoulli CPHD filter. Indeed, we obtain the multi-Bernoulli filter update equations if we set the IIDC component to be the empty set in all of these equations.

VI. AUXILIARY PARTICLE-FILTER IMPLEMENTATION

We implement the proposed filters using a Monte Carlo approach. Approximate update equations have been derived in this paper, but even they do not lead to a fully analytically tractable filter. Hence we develop particle-filter-based implementations of the filters. The basic particle-filter approach does not give a stable implementation because of the multiple approximations employed to derive the filter equations. We propose auxiliary particle-filter implementations of the multi-Bernoulli filter and the hybrid multi-Bernoulli filter based on the auxiliary particle-filter implementation of the PHD filter discussed in [39].

The normalized posterior PHD corresponding to each Bernoulli component $q_{k-1,i}(\mathbf{x})$, and the IIDC component $q_{k-1,c}(\mathbf{x})$ at time $k-1$, are approximated using a set of weighted particles as follows:

$$q_{k-1,\theta}(\mathbf{x}) \approx \hat{q}_{k-1,\theta}(\mathbf{x}) = \sum_{j=1}^{N_p} w_{k-1,\theta}^{(j)} \delta(\mathbf{x} - \mathbf{x}_{k-1,\theta}^{(j)}), \quad (64)$$

where $\theta = i, i = 1, \dots, N_{k-1}$, for Bernoulli components and $\theta = c$ for the IIDC component, and $\sum_{j=1}^{N_p} w_{k-1,\theta}^{(j)} = 1$. The probabilities of existence of the Bernoulli components are $\hat{r}_{k-1,i}$, $i = 1, \dots, N_{k-1}$, and the cardinality distribution of the IIDC component is represented using a finite dimensional vector $\hat{\pi}_{k-1}^c(n)$ whose elements sum to 1. For the hybrid multi-Bernoulli CPHD filter, the quantities $\hat{q}_{k-1,c}(\mathbf{x})$ and $\hat{\pi}_{k-1}^c(n)$ are initialized using the birth process parameters. For the CPHD filter, these quantities are obtained from the previous time step. Thus

```

1: for  $k = 1$  to  $T$  do
2:   Sample auxiliary particles
3:   Construct  $p_{k-1,\theta}(\mathbf{x})$  using (65),  $\theta = i, c$ 
4:   for  $j = 1$  to  $N_p$  do
5:     for  $i = 1$  to  $N_{k-1}$  do
6:        $\bar{\mathbf{x}}_{k-1,i}^{(j)} \sim \alpha p_{k-1,i}(\mathbf{x}) + (1-\alpha) \hat{q}_{k-1,i}(\mathbf{x})$ 
7:       Regularization:  $\bar{\mathbf{x}}_{k-1,i}^{(j)} = \bar{\mathbf{x}}_{k-1,i}^{(j)} + \Delta_{k,i}^{(j)}$ 
8:     end for
9:      $\bar{\mathbf{x}}_{k-1,c}^{(j)} \sim \alpha p_{k-1,c}(\mathbf{x}) + (1-\alpha) \hat{q}_{k-1,c}(\mathbf{x})$ 
10:    Regularization:  $\bar{\mathbf{x}}_{k-1,c}^{(j)} = \bar{\mathbf{x}}_{k-1,c}^{(j)} + \Delta_{k,c}^{(j)}$ 
11:   end for
12:   Proposal
13:   for  $j = 1$  to  $N_p$  do
14:     for  $i = 1$  to  $N_{k-1}$  do
15:        $\mathbf{x}_{k,i}^{(j)} \sim t_{k|i}(\mathbf{x}|\bar{\mathbf{x}}_{k-1,i}^{(j)})$ 
16:     end for
17:      $\mathbf{x}_{k,c}^{(j)} \sim t_{k|k-1}(\mathbf{x}|\bar{\mathbf{x}}_{k-1,c}^{(j)})$ 
18:   end for
19:    $r_{k|i} = r_{k-1,i} p_s, i = 1, 2, \dots, N_{k-1}$ 
20:   Update
21:   for  $j = 1$  to  $N_p$  do
22:     for  $i = 1$  to  $N_{k-1}$  do
23:        $w_{k,i}^{(j)} \propto w_{k-1,i}^{(j)} \frac{\mathcal{N}_{\Sigma_z + \tilde{\Sigma}_k}(\mathbf{z}_k - g(\mathbf{x}_{k,i}^{(j)}) - \tilde{\mu}_k)}{\mathcal{N}_{\Sigma_z + \Sigma_k}(\mathbf{z}_k - \mu_k)}$ 
24:     end for
25:      $w_{k,c}^{(j)} \propto w_{k-1,c}^{(j)} \frac{\mathcal{N}_{\Sigma_z + \tilde{\Sigma}_k}(\mathbf{z}_k - g(\mathbf{x}_{k,c}^{(j)}) - \tilde{\mu}_k)}{\mathcal{N}_{\Sigma_z + \Sigma_k}(\mathbf{z}_k - \mu_k)}$ 
26:   end for
27:   weight compensation  $w_{k,\theta}^{(j)} \propto \frac{w_{k,\theta}^{(j)}}{\bar{w}_{k-1,\theta}^{(j)}}$  for auxiliary particles sampled from re-weighted distribution
28:    $\{\mathbf{x}_{k,i}^{(j)}, \frac{1}{N_p}\} = \text{resample}(\{\mathbf{x}_{k,i}^{(j)}, w_{k,i}^{(j)}\}), i = 1 \dots N_{k-1}$ 
29:   Update  $r_{k,i}, i = 1 \dots N_{k-1}$  using (49)
30:   Update  $\hat{\pi}_k^c(n)$  using (61)
31:   Approximation and track management
32:   Prune Bernoulli tracks with  $r_{k,i} < r_0, i = 1 \dots N_{k-1}$ 
33:    $N_k^c = \text{MAP}(\hat{\pi}_k^c(n))$ 
34:    $\{\mathbf{x}_{k,i}^{(j)}, \frac{1}{N_p}\} = \text{split}(\{\mathbf{x}_{k,i}^{(j)}, w_{k,i}^{(j)}\}, N_k^c, r_{k,i} = 1, i = N_{k-1} + 1 \dots N_{k-1} + N_k^c)$ 
35:   Gate new Bernoulli components to check for duplicity
36: end for

```

Fig. 1. Pseudocode for auxiliary particle-filter implementation of hybrid multi-Bernoulli CPHD filter.

one particle filter is used for each Bernoulli component and one particle filter is used to approximate the IIDC component. The pseudocode for the auxiliary particle-filter implementation of the hybrid multi-Bernoulli CPHD filter is provided in Fig. 1.

For each Bernoulli component, at time k the auxiliary variables $\bar{\mathbf{x}}_{k-1,i}^{(j)}$ are sampled from a mixture of a reweighted particle set $p_{k-1,i}(\mathbf{x})$ and the posterior $\hat{q}_{k-1,i}(\mathbf{x})$ from the previous time step. Similarly for the IIDC component, the auxiliary variables $\bar{\mathbf{x}}_{k-1,c}^{(j)}$ are sampled from a mixture of a reweighted particle set $p_{k-1,c}(\mathbf{x})$ and the posterior $\hat{q}_{k-1,c}(\mathbf{x})$ from the previous time step. The

reweighted particle set $p_{k-1,\theta}(\mathbf{x})$ is given by

$$p_{k-1,\theta}(\mathbf{x}) = \sum_{j=1}^{N_p} \tilde{w}_{k-1,\theta}^{(j)} \delta(\mathbf{x} - \mathbf{x}_{k-1,\theta}^{(j)}), \quad (65)$$

$$\tilde{w}_{k-1,\theta}^{(j)} \propto w_{k-1,\theta}^{(j)} \left(\frac{\mathcal{N}_{\Sigma_z + \tilde{\Sigma}_k}(\mathbf{z}_k - g(\psi(\mathbf{x}_{k-1,\theta}^{(j)})) - \tilde{\mu}_k)}{\mathcal{N}_{\Sigma_z + \Sigma_k}(\mathbf{z}_k - \mu_k)} \right)^\epsilon, \quad (66)$$

where $\sum_{j=1}^{N_p} \tilde{w}_{k-1,\theta}^{(j)} = 1$; $\psi(\mathbf{x}_{k-1,\theta}^{(j)}) = \mathbb{E}(\mathbf{x}_{k,\theta} | \mathbf{x}_{k-1,\theta}^{(j)})$; the quantities $\tilde{\mu}_k, \tilde{\mu}_k^\theta, \tilde{\Sigma}_k,$ and $\tilde{\Sigma}_k^\theta$ are calculated using (50)–(55) and (57)–(60), with particle approximations for s_θ and v_θ evaluated using the particle set $\psi(\mathbf{x}_{k-1,\theta}^{(j)})$; and ϵ is the tempering factor [39] for stabilizing the weights in the auxiliary particle filter. Regularization is performed by adding a small zero-mean Gaussian jitter $\Delta_{k,\theta}^{(j)} \sim \mathcal{N}_{\Sigma_{\text{reg}}}(\mathbf{0})$ to the particles to maintain their diversity and avoid particle degeneracy.

In the proposal (prediction) step, the particles are propagated according to the target transition model $t_{k|k-1}(\mathbf{x}_k | \mathbf{x}_{k-1})$. For the update step, the quantities $\mu_k, \mu_k^\theta, \Sigma_k,$ and Σ_k^θ are calculated using (50)–(55) and (57)–(60). The PHD update step is realized by performing an update of the particle weights using (49) and (56). For the particles sampled from the reweighted distribution $p_{k-1,\theta}(\mathbf{x})$, weight compensation is performed. For each Bernoulli component, the weighted particle set is resampled to obtain particles with equal weights. The existence probability is updated from (49) by using particle approximation for $q_i(\mathbf{x})$. The cardinality distribution of the IIDC component $\hat{\pi}_k^c(n)$ is updated using (61)–(63).

Pruning of the Bernoulli components is performed in order to eliminate targets with low probability of existence ($< r_0$). An estimate of the number of newborn targets N_k^c is obtained from the IIDC cardinality distribution $\hat{\pi}_k^c(n)$ using the maximum a posteriori rule. The “split” function partitions the set of particles representing the normalized IIDC PHD into N_k^c clusters using the k -means algorithm, and each cluster is used to initialize a new Bernoulli component with existence probability 1. The new components created can sometimes correspond to spurious copies of existing targets; hence gating is performed so that new targets starting within close vicinity of existing targets are pruned. The definition of closeness between two targets is application dependent. We use the Euclidean distance measure between the centroids of the two particle sets representing the target positions and eliminate the new component if the distance is less than 1 m in our radio frequency tomography application. The pruned Bernoulli components are used for initialization of the IIDC PHD along with the target birth model in the next time step. This can be helpful in case of low detection probability or high noise variance.

The multi-Bernoulli auxiliary particle-filter implementation is very similar to the pseudocode given in

Fig. 1. The major difference is that instead of the IIDC component, multiple Bernoulli components are initialized in the prediction stage to account for target births. In the update stages, the PHDs of the corresponding Bernoulli components are updated. There is no clustering step required, but the pruning and gating steps are the same. The CPHD auxiliary particle-filter implementation is obtained by ignoring the steps related to the multi-Bernoulli component in Fig. 1. The normalized posterior PHD is propagated to the next time step instead of being approximated with a multi-Bernoulli component.

VII. NUMERICAL SIMULATIONS

In this section we use numerical simulations to demonstrate the application of the proposed filters to the problem of multitarget tracking. We consider two examples of the superpositional-sensor model. The first is a radio frequency tomography application, and the second is an acoustic-sensor network.

A. Target Dynamics

We assume that for each target, its dynamics are independent of the other targets and their dynamics. Specifically, the motion of each target when present within the monitoring region is governed by the following approximately constant velocity model [4]:

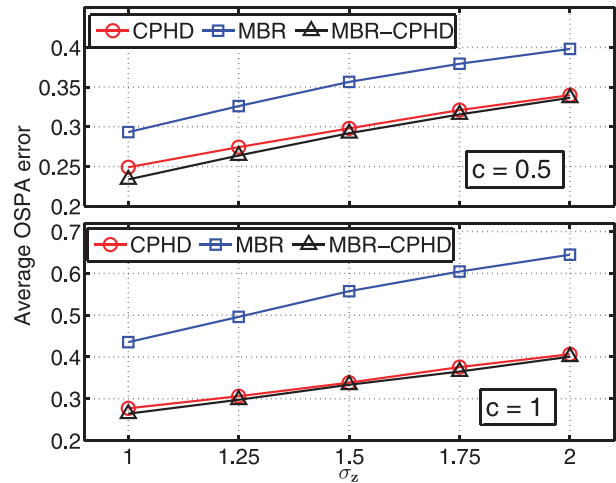
$$\mathbf{x}_{k+1,i} = \begin{bmatrix} 1 & 0 & T & 0 \\ 0 & 1 & 0 & T \\ 0 & 0 & 1 & 0 \\ 0 & 0 & 0 & 1 \end{bmatrix} \mathbf{x}_{k,i} + \begin{bmatrix} \frac{T^2}{2} & 0 \\ 0 & \frac{T^2}{2} \\ T & 0 \\ 0 & T \end{bmatrix} \begin{bmatrix} u_x \\ u_y \end{bmatrix}, \quad (67)$$

where T is the sampling period and u_x and u_y are zero-mean Gaussian white noise with respective variance $\sigma_{u_x}^2$ and $\sigma_{u_y}^2$. In this model, the state $\mathbf{x}_{k,i}$ of each object i at time k is represented by a four-dimensional vector: position on the x - and y -axis and velocity on the x - and y -axis. Multiple targets can be simultaneously present, and targets can appear or disappear over time.

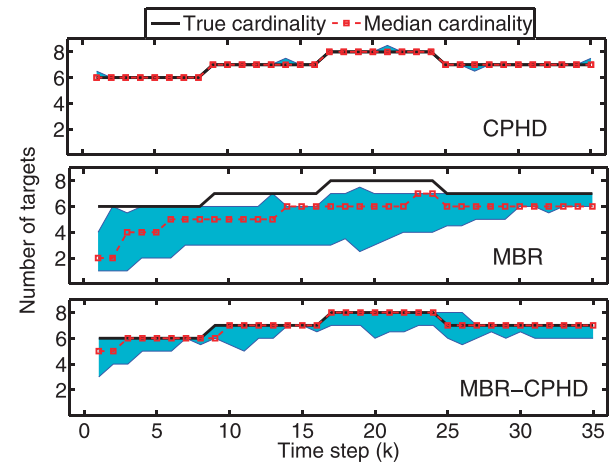
B. Radio Frequency Tomography

1) *Measurement Model:* The radio frequency (RF) tomography approach to target tracking has recently become popular [10, 40, 41]. The RF tomography measurement model we simulate here is based on work by Li et al. [41], where it is used for single-target tracking, and by Nannuru et al. [42, 43], where it is used for multitarget tracking.

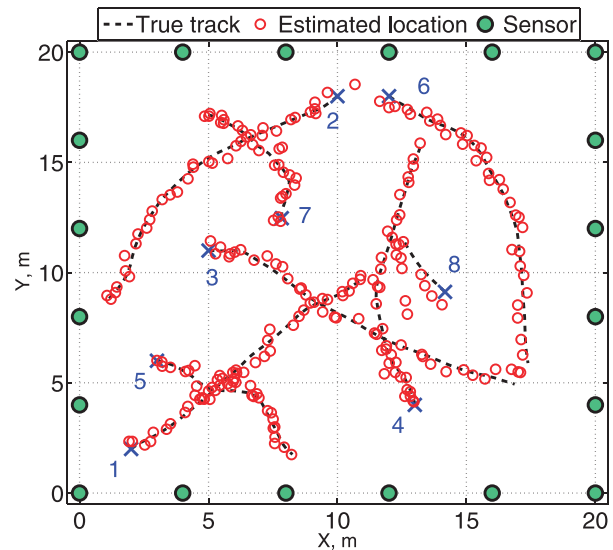
A typical deployment of RF sensors for the tomographic tracking application is shown in Fig. 2c. The measurements are the received signal strength recordings for each sensor pair. The RF sensors communicate among each other but not with the targets. A network of N_s sensors forms a total of $n_z = N_s(N_s - 1)/2$ unique sensor pairs (bidirectional links) generating n_z measurements in every time step. The background received signal strength values are recorded initially when the monitoring region is



(a) Average OSPA error



(b) Cardinality



(c) Sensor network and target tracks

Fig. 2. RF tomography. Top: Average OSPA error as measurement noise standard deviation σ_z is increased from $\sigma_z = 1$ to $\sigma_z = 2$. Middle: Median cardinality and its 5th–95th percentiles (shaded region) as function of time for $\sigma_z = 1.5$. Bottom: True target tracks and estimated target locations obtained using hybrid MBR-CPHD filter for $\sigma_z = 1.5$.

empty. The objective of RF tomography is to use the measured deviations from these background received signal strength values to track moving targets.

The empirical modeling of RF link measurements is studied in [41–43]. The j th link measurement z_k^j at time step k can be modeled as

$$z_k^j = \zeta^j(X_k) + v_k^j = \sum_{\mathbf{x} \in X_k} g^j(\mathbf{x}) + v_k^j \quad (68)$$

where

$$g^j(\mathbf{x}) = \phi \exp\left(-\frac{\lambda_j(\mathbf{x})}{\sigma_\lambda}\right) \quad (69)$$

and

$$\lambda_j(\mathbf{x}) = d_1^j(\mathbf{x}) + d_2^j(\mathbf{x}) - d_{12}^j. \quad (70)$$

Here $d_1^j(\mathbf{x})$ and $d_2^j(\mathbf{x})$ are distances between the target located at \mathbf{x} and the two sensors of link j ; d_{12}^j is the distance between the two sensors of link j ; $\lambda_j(\mathbf{x})$ is the elliptical distance measure between a target located at \mathbf{x} and link j (see [41] for more details); ϕ and σ_λ are fixed parameters based on physical properties of the sensors and targets; and v_k^j is the zero-mean Gaussian sensor noise. The RF tomography measurement equation has a superpositional form, as can be seen by comparing (68) with (2).

We simulate an RF sensor network with $N_s = 20$ sensor nodes distributed uniformly on the periphery of the 20 m \times 20 m square region as shown in Fig. 2c. This gives rise to a total of $n_z = 190$ unique bidirectional links. The observation-model parameters are $\phi = 5$ and $\sigma_\lambda = 0.4$. The measurement noise variance is $\Sigma_z = \sigma_z^2 I_{n_z}$, where I_{n_z} is the $n_z \times n_z$ identity matrix.

2) *Motion-Model Parameters:* Fig. 2c shows the target tracks we use for the simulations. The black cross (\times) indicates the starting location of the target. The variation of number of targets over time is shown in Fig. 2b. The targets labeled 7 and 8 in Fig. 2c appear within the monitoring region at time steps 9 and 17, respectively. Target 8 disappears from the monitoring region at time step 24. The targets in this scenario evolve according to the linear Gaussian dynamics given in (67) with a time step of duration $T = 0.25$ s and the noise variance parameters of $\sigma_{u_x}^2 = \sigma_{u_y}^2 = 0.35$. We simulate 35 time steps of target motion for a total of $35 \times 0.25 = 8.75$ s.

3) *Error Metric and Filter Settings:* We compare the multi-Bernoulli (MBR) filter and the hybrid multi-Bernoulli CPHD (MBR-CPHD) filter with the CPHD filter. The auxiliary particle-filter implementations of these filters are as discussed in Section VI. To compare them, we need to find the error between the filter estimates and the true multitarget state. Since we have to compare sets, possibly with different cardinality, we use the optimal subpattern assignment (OSPA) metric [44]. The OSPA metric penalizes errors in estimating target location as well as in estimating the number of targets using the cardinality penalty factor c . The multitarget state estimate is obtained by averaging particles representing position for

each existing Bernoulli component. For the CPHD filter, the state estimates are centroids of the clusters obtained by partitioning the particle set using the k -means algorithm.

A single target survival probability is assumed to be constant throughout the monitoring region and is equal to $p_s = 0.9$. For the MBR filter, four new Bernoulli components are added at each time step to account for target births. The probability of existence of these new components is $r^B = 0.2$, and their density functions are uniform within the monitoring region. For the hybrid MBR-CPHD filter, the birth process is IIDC with discrete uniform cardinality distribution and the normalized PHD is assumed uniform within the monitoring region. Rejected components from the current time step are also used to partially initialize the PHD of the IIDC component in the next time step. This way, targets with low probability of existence which get erroneously eliminated can be reintroduced using the IIDC component.

Spurious new Bernoulli components often get initialized near existing target locations. We prune these duplicate components by performing gating with a gating radius of 1 m. Bernoulli components with existence probability lower than the existence probability at birth are pruned—i.e., $r_0 = r^B = 0.2$. A low existence probability threshold is chosen because it can identify individual targets even when they are in close vicinity. We use $N_p = 1000$ particles for each particle filter. In the auxiliary step we use $\alpha = 0.5$ and the tempering factor is $\epsilon = 0.3$. For regularization of particles we set $\Sigma_{\text{reg}} = \sigma_{\text{reg}}^2 \text{diag}(1, 1, 1, 1)$ with $\sigma_{\text{reg}} = 0.25$.

4) *Simulation Results:* The average OSPA error metrics are calculated by repeating simulations multiple times with different random initializations. The target tracks shown in Fig. 2c are used for all the Monte Carlo runs. A set of 20 different measurement sequences is generated and each is processed with five different random initializations for all the algorithms. Thus the average error is reported by running 100 Monte Carlo simulations. We ignore the first five time steps when calculating the average error, to allow the filter estimates to stabilize. The mean OSPA error is calculated for different values of the measurement noise parameter σ_z and is shown in Fig. 2a for $c = 0.5$ and $c = 1$. As the noise is increased from $\sigma_z = 1$ to $\sigma_z = 2$, the performance of all the filters deteriorates. When the measurement noise is small, the hybrid MBR-CPHD filter has the lowest error among all the filters. For higher measurement noise, the CPHD filter and the hybrid MBR-CPHD filter have almost the same performance.

The median cardinality estimates (over the 100 Monte Carlo simulations) and the 5th and 95th percentiles for the different algorithms are shown in Fig. 2b for $\sigma_z = 1.5$. The multi-Bernoulli filter has low initial cardinality estimates because only a maximum of four new Bernoulli components are added at each time step. The MBR filter also significantly underestimates the number of targets, which is reflected as high average OSPA error, as seen from Fig. 2a. The CPHD filter has the most accurate

cardinality estimate, as its 5th and 95th percentiles coincide with the median cardinality at most of the time steps. The hybrid MBR-CPHD filter makes significantly better cardinality estimates than the MBR filter. The targets missed by the MBR-CPHD filter at the current time step are reintroduced by input from the CPHD component at the next time step. Since the average OSPA error for the CPHD filter and the MBR-CPHD filter are almost the same and the CPHD filter provides better cardinality estimates than the MBR-CPHD filter, the MBR-CPHD filter provides more accurate target location information than the CPHD filter. In fact, ignoring the errors in cardinality, the root mean square error averaged over 100 Monte Carlo simulations is 0.42, 0.54, and 0.32 m for the CPHD, MBR, and MBR-CPHD filters, respectively, when the measurement noise is $\sigma_z = 1.5$. Fig. 2c depicts an example of target location estimates obtained using the hybrid MBR-CPHD filter.

C. Acoustic-Sensor Network

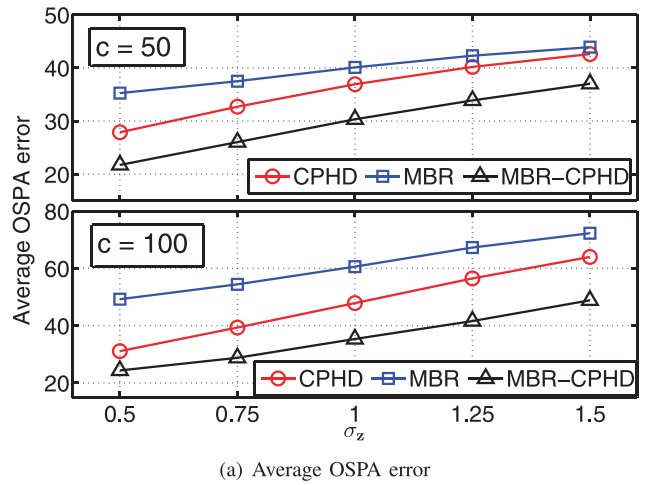
1) *Measurement Model:* Acoustic-sensor networks can be used for multitarget tracking based on the strength of the emitted acoustic signals. In this paper we adapt the acoustic amplitude-sensor measurement model discussed in [9]. A possible deployment of an acoustic-sensor network is shown in Fig. 3c. It is an active tracking system in which each target emits an acoustic signal of known amplitude A and all the sensors receive the signal. If a target at location \mathbf{x} emits the acoustic signal, a sensor located at d^j receives the signal at a reduced strength of $gd^j(\mathbf{x}) = A/\max(\|\mathbf{x} - d^j\|, d_0)^\kappa$, where $\|\mathbf{x}\|$ denotes the Euclidean norm of vector \mathbf{x} , κ is the path loss exponent, and d_0 is the threshold distance such that the received signal amplitude saturates if the target is closer than d_0 of the sensor. When multiple targets are present, the strength of the combined signal received by each of the sensors is the sum of the strength of the signals due to each of the individual targets. Thus the measurement z_k^j received by sensor j at time k can be modeled as

$$z_k^j = \zeta^j(X_k) + v_k^j \quad (71)$$

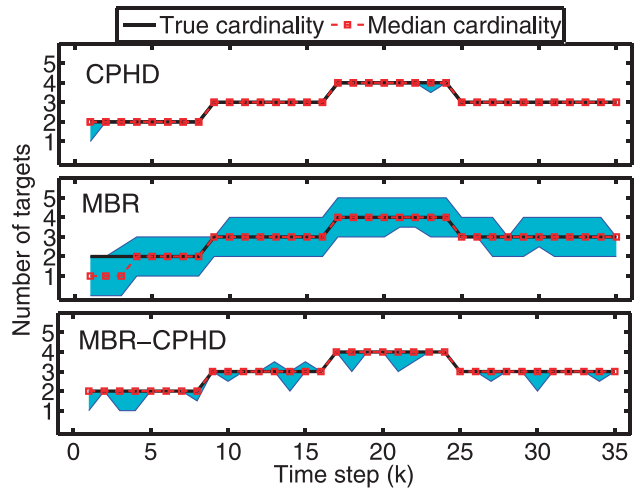
$$= \sum_{\mathbf{x} \in X_k} \frac{A}{\max(\|\mathbf{x} - d^j\|, d_0)^\kappa} + v_k^j, \quad (72)$$

where v_k^j is the zero-mean Gaussian measurement noise. This measurement model is of the superpositional form, as can be seen by comparing (72) with (2).

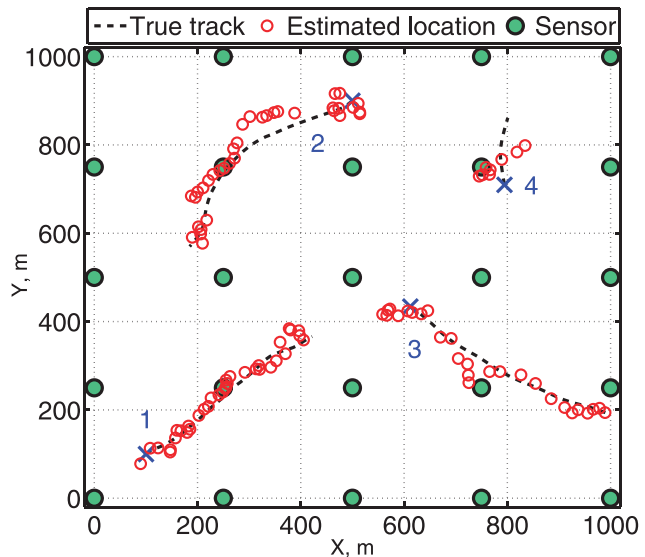
We simulate an acoustic-sensor network with $N_s = 25$ sensor nodes distributed in a 1000 m \times 1000 m square region in a grid format, as shown in Fig. 3c. A wider observation region is chosen to evaluate the robustness of the filters in a more challenging scenario. The measurement dimension is $n_z = N_s = 25$, and the measurement-model parameters are $A = 500$, $\kappa = 1$, and $d_0 = 1$. The measurement noise variance is $\Sigma_z = \sigma_z^2 I_{n_z}$.



(a) Average OSPA error



(b) Cardinality



(c) Sensor network and target tracks

Fig. 3. Acoustic-sensor network. Top: Average OSPA error as measurement noise standard deviation σ_z is increased from $\sigma_z = 0.5$ to $\sigma_z = 1.5$. Middle: Median cardinality and its 5th–95th percentiles (shaded region) as function of time for $\sigma_z = 1$. Bottom: True target tracks and estimated target locations obtained using MBR-CPHD filter for $\sigma_z = 1$.

TABLE I
Average Computational Time (in Seconds) Required to Process One
Observation Vector for $\sigma_z = 1$

Algorithm	Average Computational Time	
	RF Tomography	Acoustic Network
CPHD	3.76	0.73
MBR	2.54	0.63
MBR-CPHD	2.41	0.58

2) Motion-Model Parameters and Filter Settings:

The target dynamics discussed in Section VII-A are used to simulate the target tracks. The simulated target tracks are shown in Fig. 3c, and the target number variation is shown in Fig. 3b. These tracks are simulated for 35 time steps using the process noise parameters of $\sigma_{u_x} = \sigma_{u_y} = 25$ m and time-step duration $T = 0.25$ s. Most of the filter settings are the same as those discussed in Section VII-B-3. The gating radius is increased to 100 m, since the monitored region is considerably larger.

3) *Simulation Results:* Fig. 3a shows how the average OSPA error varies as a function of measurement noise for $c = 50$ and $c = 100$. The averages are calculated using 100 Monte Carlo simulations. The hybrid MBR-CPHD filter performs significantly better than the CPHD filter in this setup and has the lowest average OSPA error for all values of σ_z . The median cardinality and the 5th and 95th percentiles are shown in Fig. 3b for $\sigma_z = 1$. The CPHD filter has the most accurate cardinality estimates, followed by the hybrid MBR-CPHD filter and the MBR filter. Since the hybrid MBR-CPHD filter has lower average OSPA error than the CPHD filter, for the targets that are correctly identified, the hybrid MBR-CPHD filter is able to accurately track their locations in a much wider observation region. Fig. 3c shows the true target trajectories and the estimated target locations obtained using the hybrid MBR-CPHD filter for $\sigma_z = 1$.

D. Computational Requirements

Table I compares the average computational time² required for the different algorithms to process one observation vector. The time required to process one observation vector of the acoustic-sensor network is much smaller than that of the RF-sensor network because the measurement dimension is much smaller and there are fewer targets. The hybrid MBR-CPHD filter is the fastest of the filters. The CPHD filter has higher computational requirements because of the costly clustering step required at each time step, and the MBR filter has higher computational requirements because of the multiple additional particle filters employed to account for new target arrivals. The hybrid MBR-CPHD filter saves computation by initiating new particle filters only if the

² All the simulations were performed using algorithms implemented in MATLAB on Two Xeon four-core 2.5 GHz computers with 14 GB of RAM.

IIDC component indicates arrival of new targets, and the costly clustering step is required only when multiple new targets arrive within the monitoring region in the same time step.

VIII. CONCLUSIONS

We studied the multi-Bernoulli filter and the hybrid multi-Bernoulli CPHD filter for a superpositional-sensor model in this paper. The methodology for deriving update equations is similar for both the filters and is based on propagating the PHD of individual RFS components. The cardinality distribution is additionally propagated for the hybrid multi-Bernoulli CPHD filter. We proposed auxiliary particle-filter implementations of the filters and conducted a numerical study using a simulated RF tomography setup and an acoustic-sensor network setup to perform multitarget tracking. The hybrid multi-Bernoulli CPHD filter performed better than the multi-Bernoulli filter and better than or equal to the CPHD filter when using the OSPA-error metric. The hybrid filter was the least computationally demanding.

APPENDIX A. APPLICATION OF CAMPBELL'S THEOREM

Let $f(W)$ be a multitarget density corresponding to some random finite set. Denote the PHD function and the second factorial moment density function of the RFS by $D(\mathbf{x})$ and $D(\mathbf{x}_1, \mathbf{x}_2)$ respectively. Let the random vector \mathbf{y} be a function defined over random sets as $\mathbf{y} = r(W) = \sum_{\mathbf{w} \in W} g(\mathbf{w})$. Then according to the quadratic version of Campbell's theorem [24, 25],

$$\mu = E[(\mathbf{y})] = \int g(\mathbf{x}) D(\mathbf{x}) d\mathbf{x} \quad (73)$$

and

$$\begin{aligned} \Sigma = E[(\mathbf{y} - \mu)(\mathbf{y} - \mu)^T] &= \int g(\mathbf{x}) g(\mathbf{x})^T D(\mathbf{x}) d\mathbf{x} \\ &+ \iint g(\mathbf{x}_1) g(\mathbf{x}_2)^T \tilde{D}(\{\mathbf{x}_1, \mathbf{x}_2\}) d\mathbf{x}_1 d\mathbf{x}_2, \end{aligned} \quad (74)$$

where $\tilde{D}(\{\mathbf{x}_1, \mathbf{x}_2\}) = D(\{\mathbf{x}_1, \mathbf{x}_2\}) - D(\mathbf{x}_1)D(\mathbf{x}_2)$. Thus the mean and covariance matrix, which represent the first- and second-order statistics of the random vector \mathbf{y} , depend on the PHD function and the second factorial moment density function of the corresponding random set.

A. Multi-Bernoulli RFS

For the multi-Bernoulli distribution, substituting (13) and (15) into (73) and (74) yields

$$\mu_{k+1} = \int g(\mathbf{x}) \left(\sum_{i=1}^{N_{k+1|k}} r_i q_i(\mathbf{x}) \right) d\mathbf{x} \quad (75)$$

$$= \sum_{i=1}^{N_{k+1|k}} r_i \int g(\mathbf{x}) q_i(\mathbf{x}) d\mathbf{x} = \sum_{i=1}^{N_{k+1|k}} r_i s_i \quad (76)$$

and

$$\begin{aligned}\Sigma_{k+1} &= \int g(\mathbf{x})g(\mathbf{x})^T \left(\sum_{i=1}^{N_{k+1|k}} r_i q_i(\mathbf{x}) \right) d\mathbf{x} \\ &\quad - \iint g(\mathbf{x}_1)g(\mathbf{x}_2)^T \left(\sum_{i=1}^{N_{k+1|k}} r_i^2 q_i(\mathbf{x}_1)q_i(\mathbf{x}_2) \right) d\mathbf{x}_1 d\mathbf{x}_2\end{aligned}\quad (77)$$

$$= \sum_{i=1}^{N_{k+1|k}} (r_i v_i - r_i^2 s_i s_i^T), \quad (78)$$

where

$$s_i = \langle q_i, g \rangle, \quad v_i = \langle q_i, g g^T \rangle. \quad (79)$$

We now consider the multi-Bernoulli RFS $\Xi_{k+1|k}$ with $N_{k+1|k}$ parameters to be the union of a Bernoulli RFS $\Xi_{k+1|k}^A$ with parameters $\{r_i, q_i(\mathbf{x})\}$ and another multi-Bernoulli RFS $\Xi_{k+1|k}^B$ with the remaining parameter set $\{r_j, q_j(\mathbf{x})\}_{j \neq i}$. The density $f_{k+1|k}^{A*}(W)$ in (26) can be interpreted as the multitarget distribution of the RFS, which is the union of independent random finite sets with multitarget densities given by $f_{k+1|k}^{A_x}(W)$ and $f_{k+1|k}^B(W)$, where $f_{k+1|k}^{A_x}(W)$ is defined in (25). From (12), the density function $f_{k+1|k}^{A_x}(W)$ corresponds to an RFS which is empty with probability 1, and hence all its moments are zero. Hence the parameters $\mu_{k+1}^{A_x}$ and $\Sigma_{k+1}^{A_x}$, using Campbell's theorem, are

$$\mu_{k+1}^{A_x} = 0 + \sum_{j=1, j \neq i}^{N_{k+1|k}} r_j s_j \quad (80)$$

$$= \mu_{k+1} - r_i s_i = \mu_{k+1}^{\bar{i}} \quad (81)$$

and

$$\Sigma_{k+1}^{A_x} = 0 + \sum_{j=1, j \neq i}^{N_{k+1|k}} (r_j v_j - r_j^2 s_j s_j^T) \quad (82)$$

$$= \Sigma_{k+1} - (r_i v_i - r_i^2 s_i s_i^T) = \Sigma_{k+1}^{\bar{i}}. \quad (83)$$

B. Union of Multi-Bernoulli RFS and IIDC RFS

Let the RFS Ξ be the union of a multi-Bernoulli RFS with parameters $\{r_i, q_i(\mathbf{x})\}_{i=1}^{N_{k+1|k}}$ and an IIDC RFS with parameters $\{q_c(\mathbf{x}), \pi^c(n)\}$. Using the expression for PHD and second factorial moments from (8), (10), (13), and (15), we have

$$\mu_{k+1} = \int g(\mathbf{x}) \left(\sum_{i=1}^{N_{k+1|k}} r_i q_i(\mathbf{x}) + \mu_c q_c(\mathbf{x}) \right) d\mathbf{x} \quad (84)$$

$$= \sum_{i=1}^{N_{k+1|k}} r_i s_i + \mu_c s_c \quad (85)$$

and

$$\begin{aligned}\Sigma_{k+1} &= \int g(\mathbf{x})g(\mathbf{x})^T \left(\sum_{i=1}^{N_{k+1|k}} r_i q_i(\mathbf{x}) + \mu_c q_c(\mathbf{x}) \right) d\mathbf{x} \\ &\quad - \iint g(\mathbf{x}_1)g(\mathbf{x}_2)^T \left(\sum_{i=1}^{N_{k+1|k}} r_i^2 q_i(\mathbf{x}_1)q_i(\mathbf{x}_2) \right) d\mathbf{x}_1 d\mathbf{x}_2 \\ &\quad + \iint g(\mathbf{x}_1)g(\mathbf{x}_2)^T (a - \mu_c^2) q_c(\mathbf{x}_1)q_c(\mathbf{x}_2) d\mathbf{x}_1 d\mathbf{x}_2\end{aligned}\quad (86)$$

$$= \sum_{i=1}^{N_{k+1|k}} (r_i v_i - r_i^2 s_i s_i^T) + \mu_c v_c - (\mu_c^2 - a) s_c s_c^T, \quad (87)$$

where

$$s_c = \langle q_c, g \rangle, \quad v_c = \langle q_c, g g^T \rangle. \quad (88)$$

We now consider the random finite set $\Xi_{k+1|k}$ to be the union of three independent random finite sets as follows: $\Xi_{k+1|k} = \Xi_{k+1|k}^A \cup \Xi_{k+1|k}^B \cup \Xi_{k+1|k}^C$. Let $\Xi_{k+1|k}^A$ be a Bernoulli RFS with parameters $\{r_i, q_i(\mathbf{x})\}$, $\Xi_{k+1|k}^B$ be a multi-Bernoulli RFS with parameter set $\{r_j, q_j(\mathbf{x})\}_{j \neq i}$, and $\Xi_{k+1|k}^C$ be an IIDC RFS with parameters $\{q_c(\mathbf{x}), \pi^c(n)\}$. The density $f_{k+1|k}^{A*}(W)$ in (26) can be interpreted to be the density of an RFS which is the union of three independent random finite sets. From (12), the density function $f_{k+1|k}^{A_x}(W)$ corresponds to an RFS which is empty with probability 1, and hence all its moments are zero. The parameters $\mu_{k+1}^{A_x}$ and $\Sigma_{k+1}^{A_x}$, therefore, using Campbell's theorem, are

$$\mu_{k+1}^{A_x} = 0 + \sum_{j=1, j \neq i}^{N_{k+1|k}} r_j s_j + \mu_c s_c \quad (89)$$

$$= \mu_{k+1} - r_i s_i = \mu_{k+1}^{\bar{i}} \quad (90)$$

and

$$\begin{aligned}\Sigma_{k+1}^{A_x} &= 0 + \sum_{j=1, j \neq i}^{N_{k+1|k}} (r_j v_j - r_j^2 s_j s_j^T) \\ &\quad + \mu_c v_c - (\mu_c^2 - a) s_c s_c^T\end{aligned}\quad (91)$$

$$= \Sigma_{k+1} - (r_i v_i - r_i^2 s_i s_i^T) = \Sigma_{k+1}^{\bar{i}}. \quad (92)$$

We now consider the random finite set $\Xi_{k+1|k}$ to be the union of two independent random finite sets as follows: $\Xi_{k+1|k} = \Xi_{k+1|k}^A \cup \Xi_{k+1|k}^B$. Let $\Xi_{k+1|k}^A$ be an IIDC RFS with parameters $\{q_c(\mathbf{x}), \pi^c(n)\}$ and $\Xi_{k+1|k}^B$ be a multi-Bernoulli RFS with parameter set $\{r_j, q_j(\mathbf{x})\}_{j=1}^{N_{k+1|k}}$. In this case the multitarget density $f_{k+1|k}^{A_x}(W)$ corresponds to an IIDC RFS with parameters $\{q_c(\mathbf{x}), [(n+1)\pi^c(n+1)]/\mu_c\}$ with probability 1. This is

because, when $\mathbf{x} \notin W$ (event with probability 1), we have

$$f_{k+1|k}^{A_{\mathbf{x}}}(W) = \frac{f_{k+1|k}^A(\{\mathbf{x}\} \cup W)}{D_{k+1|k}^A(\mathbf{x})} \quad (93)$$

$$= \frac{(|W| + 1)! \pi^c (|W| + 1) q_c^{\{\mathbf{x}\} \cup W}}{\mu_c q_c(\mathbf{x})} \quad (94)$$

$$= \frac{(|W| + 1)! \pi^c (|W| + 1) q_c^W}{\mu_c} \quad (95)$$

$$= |W|! \frac{(|W| + 1) \pi^c (|W| + 1)}{\mu_c} q_c^W. \quad (96)$$

The μ_c and a parameters corresponding to the cardinality distribution $[(n + 1)\pi^c(n + 1)]/\mu_c$ are a/μ_c and b/μ_c , respectively. Thus from (85) and (87) we have

$$\mu_{k+1}^{A_{\mathbf{x}}} = \sum_{j=1}^{N_{k+1|k}} r_j s_j + \frac{a}{\mu_c} s_c = \mu_{k+1}^{\bar{c}} \quad (97)$$

and

$$\Sigma_{k+1}^{A_{\mathbf{x}}} = \sum_{j=1}^{N_{k+1|k}} (r_j v_j - r_j^2 s_j s_j^T) + \frac{a}{\mu_c} v_c - \left(\frac{a^2}{\mu_c^2} - \frac{b}{\mu_c} \right) s_c s_c^T \quad (98)$$

$$= \Sigma_{k+1}^{\bar{c}}. \quad (99)$$

APPENDIX B. CARDINALITY UPDATE FOR IIDC COMPONENT

We now derive the cardinality distribution of the posterior IIDC component. This can be defined as

$$\pi_{k+1}^c(n) = \int_{|W|^c=n} f_{k+1|k+1}(W) \delta W \quad (100)$$

$$= \frac{\int_{|W|^c=n} h_{\mathbf{z}_{k+1}}(W) f_{k+1|k}(W) \delta W}{\int h_{\mathbf{z}_{k+1}}(W) f_{k+1|k}(W) \delta W} \quad (101)$$

$$= \pi_{k+1|k}^c(n) \frac{\int h_{\mathbf{z}_{k+1}}(W) f_{k+1|k}^{c,n}(W) \delta W}{\int h_{\mathbf{z}_{k+1}}(W) f_{k+1|k}(W) \delta W}, \quad (102)$$

where

$$f_{k+1|k}^{c,n}(W) = \frac{1}{\pi_{k+1|k}^c(n)} \delta_{|W|^c}(n) f_{k+1|k}(W). \quad (103)$$

The multitarget density $f_{k+1|k}^{c,n}(W)$ corresponds to the union of a multi-Bernoulli RFS and the random finite set obtained by constraining the cardinality ($|W|^c = n$) of the IIDC RFS. Applying the approximations as before, we get

$$\pi_{k+1}^c(n) \approx \pi_{k+1|k}^c(n) \frac{\mathcal{N}_{\Sigma_{\mathbf{z}} + \Sigma_{k+1}^{c,n}}(\mathbf{z}_{k+1} - \mu_{k+1}^{c,n})}{\mathcal{N}_{\Sigma_{\mathbf{z}} + \Sigma_{k+1}}(\mathbf{z}_{k+1} - \mu_{k+1})}, \quad (104)$$

where μ_{k+1} and Σ_{k+1} are as given in (85) and (87). From [24, 25] we have

$$\mu_{k+1}^{c,n} = \sum_{i=1}^{N_{k+1|k}} r_i s_i + n s_c \quad (105)$$

and

$$\Sigma_{k+1}^{c,n} = \sum_{i=1}^{N_{k+1|k}} (r_i v_i - r_i^2 s_i s_i^T) + n (v_c - s_c s_c^T). \quad (106)$$

Note that in this update equation there is no assumption made about the cardinality of the multi-Bernoulli component.

REFERENCES

- [1] Mahler, R. P. S. *Statistical Multisource-Multitarget Information Fusion*. Norwood, MA: Artech House, 2007.
- [2] Mahler, R. P. S. Multitarget Bayes filtering via first-order multitarget moments. *IEEE Transactions on Aerospace and Electronic Systems*, **39**, 4 (Oct. 2003), 1152–1178.
- [3] Mahler, R. PHD filters of higher order in target number. *IEEE Transactions on Aerospace and Electronic Systems*, **43**, 4 (Oct. 2007), 1523–1543.
- [4] Vo, B.-N., Singh, S., and Doucet, A. Sequential Monte Carlo methods for multitarget filtering with random finite sets. *IEEE Transactions on Aerospace and Electronic Systems*, **41**, 4 (Oct. 2005), 1224–1245.
- [5] Mahler, R. CPHD filters for superpositional sensors. *Proceedings of SPIE*, **7445** (Sept. 2009), 74450E.
- [6] Balakumar, B., Sinha, A., Kirubarajan, T., and Reilly, J. P. PHD filtering for tracking an unknown number of sources using an array of sensors. In *IEEE/SP 13th Workshop on Statistical Signal Processing*, Bordeaux, France, July 2005.
- [7] Angelosante, D., Biglieri, E., and Lops, M. Multiuser detection in a dynamic environment: Joint user identification and parameter estimation. In *IEEE International Symposium on Information Theory*, Nice, France, June 2007.
- [8] Angelosante, D., Biglieri, E., and Lops, M. Sequential estimation of multipath MIMO-OFDM channels. *IEEE Transactions on Signal Processing*, **57**, 8 (Aug. 2009), 3167–3181.
- [9] Hlinka, O., Slučiak, O., Hlawatsch, F., Djuric, P. M., and Rupp, M. Likelihood consensus and its application to distributed particle filtering. *IEEE Transactions on Signal Processing*, **60**, 8 (Aug. 2012), 4334–4349.
- [10] Wilson, J., and Patwari, N. Radio tomographic imaging with wireless networks. *IEEE Transactions on Mobile Computing*, **9**, 5 (May 2010), 621–632.
- [11] Battistelli, G., Chisci, L., Morrocchi, S., Papi, F., Farina, A., and Graziano, A. Robust multisensor multitarget tracker with application to passive multistatic radar tracking. *IEEE Transactions on Aerospace and Electronic Systems*, **48**, 4 (Oct. 2012), 3450–3472.
- [12] Mullane, J., Vo, B.-N., Adams, M. D., and Vo, B.-T. A random-finite-set approach to Bayesian SLAM. *IEEE Transactions on Robotics*, **27**, 2 (Apr. 2011), 268–282.
- [13] Battistelli, G., Chisci, L., Fantacci, C., Farina, A., and Graziano, A.

- Consensus CPHD filter for distributed multitarget tracking. *IEEE Journal of Selected Topics in Signal Processing*, **7**, 3 (June 2013), 508–520.
- [14] Vo, B.-T., Vo, B.-N., and Cantoni, A. The cardinality balanced multi-target multi-Bernoulli filter and its implementations. *IEEE Transactions on Signal Processing*, **57**, 2 (Feb. 2009), 409–423.
- [15] Vo, B.-T., and Vo, B.-N. Labeled random finite sets and multi-object conjugate priors. *IEEE Transactions on Signal Processing*, **61**, 13 (July 2013), 3460–3475.
- [16] Vo, B.-N., Vo, B.-T., and Phung, D. Labeled random finite sets and the Bayes multi-target tracking filter. *IEEE Transactions on Signal Processing*, **62**, 24 (Dec. 2014), 6554–6567.
- [17] Reuter, S., Vo, B.-T., Vo, B.-N., and Dietmayer, K. The labeled multi-Bernoulli filter. *IEEE Transactions on Signal Processing*, **62**, 12 (June 2014), 3246–3260.
- [18] Fantacci, C., Vo, B.-T., Papi, F., and Vo, B.-N. (2015 January). The marginalized δ -GLMB filter. [Online]. <http://arxiv.org/abs/1501.00926>.
- [19] Nannuru, S., and Coates, M. Multi-Bernoulli filter for superpositional sensors. In *16th International Conference on Information Fusion*, Istanbul, Turkey, July 2013.
- [20] Nannuru, S., and Coates, M. Hybrid multi-Bernoulli CPHD filter for superpositional sensors. *Proceedings of SPIE*, **9091** (June 2014), 90910D.
- [21] Mahler, R. P. S. *Advances in Statistical Multisource-Multitarget Information Fusion*. Norwood, MA: Artech House, 2014.
- [22] Thouin, F., Nannuru, S., and Coates, M. Multi-target tracking for measurement models with additive contributions. In *Proceedings of the 14th International Conference on Information Fusion*, Chicago, IL, July 2011.
- [23] Thouin, F., Nannuru, S., and Coates, M. (2011 July). Multi-target tracking for measurement models with additive contributions. [Online]. <http://networks.ece.mcgill.ca/node/189>.
- [24] Mahler, R., and El-Fallah, A. An approximate CPHD filter for superpositional sensors. *Proceedings of SPIE*, **8392** (May 2012), 83920K.
- [25] Nannuru, S., Coates, M., and Mahler, R. Computationally-tractable approximate PHD and CPHD filters for superpositional sensors. *IEEE Journal of Selected Topics in Signal Processing*, **7**, 3 (June 2013), 410–420.
- [26] Hauschildt, D. Gaussian mixture implementation of the cardinalized probability hypothesis density filter for superpositional sensors. In *2011 International Conference on Indoor Positioning and Indoor Navigation*, Guimaraes, Portugal, Sept. 2011.
- [27] Hoseinnezhad, R., Vo, B.-N., Vo, B.-T., and Suter, D. Visual tracking of numerous targets via multi-Bernoulli filtering of image data. *Pattern Recognition*, **45**, 10 (Oct. 2012), 3625–3635.
- [28] Hoseinnezhad, R., Vo, B.-N., and Vo, B.-T. Visual tracking in background subtracted image sequences via multi-Bernoulli filtering. *IEEE Transactions on Signal Processing*, **61**, 2 (Jan. 2013), 392–397.
- [29] Nannuru, S., and Coates, M. Particle filter implementation of the multi-Bernoulli filter for superpositional sensors. In *IEEE 5th International Workshop on Computational Advances in Multi-Sensor Adaptive Processing*, Saint Martin, Dec. 2013.
- [30] Djuric, P. M., Lu, T., and Bugallo, M. F. Multiple particle filtering. In *IEEE International Conference on Acoustics, Speech and Signal Processing*, Honolulu, HI, June 2007.
- [31] Papi, F., and Kim, D. Y. (2014 December). A particle multi-target tracker for superpositional measurements using labeled random finite sets. [Online]. <http://arxiv.org/abs/1501.02248>.
- [32] Papi, F., Vo, B.-N., Vo, B.-T., Fantacci, C., and Beard, M. (2014 December). Generalized labeled multi-Bernoulli approximation of multi-object densities. [Online]. <http://arxiv.org/abs/1412.5294>.
- [33] Beard, M., Vo, B.-T., and Vo, B.-N. Bayesian multi-target tracking with merged measurements using labelled random finite sets. *IEEE Transactions on Signal Processing*, **63**, 6 (Mar. 2015), 1433–1447.
- [34] Williams, J. L. Hybrid Poisson and multi-Bernoulli filters. In *15th International Conference on Information Fusion*, Singapore, July 2012.
- [35] Pollard, E., Pannetier, B., and Rombaut, M. Hybrid algorithms for multitarget tracking using MHT and GM-CPHD. *IEEE Transactions on Aerospace and Electronic Systems*, **47**, 2 (Apr. 2011), 832–847.
- [36] Panta, K., Vo, B.-N., and Singh, S. Novel data association schemes for the probability hypothesis density filter. *IEEE Transactions on Aerospace and Electronic Systems*, **43**, 2 (Apr. 2007), 556–570.
- [37] Nannuru, S., and Coates, M. J. (2015 February). Technical report: Gaussian approximation for superpositional sensors. <http://networks.ece.mcgill.ca/node/349>.
- [38] Vo, B.-N., Vo, B.-T., Pham, N.-T., and Suter, D. Joint detection and estimation of multiple objects from image observations. *IEEE Transactions on Signal Processing*, **58**, 10 (Oct. 2010), 5129–5141.
- [39] Whiteley, N., Singh, S., and Godsill, S. Auxiliary particle implementation of probability hypothesis density filter. *IEEE Transactions on Aerospace and Electronic Systems*, **46**, 3 (July 2010), 1437–1454.
- [40] Zhang, D., Ma, J., Chen, Q., and Ni, L. M. An RF-based system for tracking transceiver-free objects. In *Fifth Annual IEEE International Conference on Pervasive Computing and Communications*, White Plains, NY, Mar. 2007.
- [41] Li, Y., Chen, X., Coates, M., and Yang, B. Sequential Monte Carlo radio-frequency tomographic tracking. In *2011 IEEE International Conference on Acoustics, Speech and Signal Processing*, Prague, Czech Republic, May 2011.
- [42] Nannuru, S., Li, Y., Coates, M., and Yang, B. Multi-target device-free tracking using radio frequency tomography. In *Seventh International Conference on Intelligent Sensors, Sensor Networks and Information Processing*, Adelaide, Australia, Dec. 2011.

- [43] Nannuru, S., Li, Y., Zeng, Y., Coates, M., and Yang, B. Radio-frequency tomography for passive indoor multitarget tracking. *IEEE Transactions on Mobile Computing*, **12**, 12 (Dec. 2013), 2322–2333.
- [44] Schuhmacher, D., Vo, B.-T., and Vo, B.-N. A consistent metric for performance evaluation of multi-object filters. *IEEE Transactions on Signal Processing*, **56**, 8 (Aug. 2008), 3447–3457.



Santosh Nannuru is currently pursuing his doctoral studies in electrical engineering at McGill University, Canada. He received both his B.Tech. and M.Tech. degrees in electrical engineering from the Indian Institute of Technology, Bombay, in 2009. He worked as a design engineer at iKoa Semiconductors for a year before starting his Ph.D. degree studies. He is a recipient of the McGill Engineering Doctoral Award. His research interests are in signal processing, Bayesian inference, Monte Carlo methods, and the random-finite-set approach to filtering.



Mark Coates received a B.E. degree (first-class honor) in computer systems engineering from the University of Adelaide, Australia, in 1995, and a Ph.D. degree in information engineering from the University of Cambridge, United Kingdom, in 1999. He joined McGill University (Montreal, Canada) in 2002, where he is currently an associate professor in the department of electrical and computer engineering. He was awarded the Texas Instruments Postdoctoral Fellowship in 1999 and was a research associate and lecturer at Rice University, Texas, from 1999 through 2001. He was an associate editor of *IEEE Transactions on Signal Processing* from 2007 through 2011 and is currently a senior area editor of *IEEE Signal Processing Letters*. His research interests include communication and sensor networks, statistical signal processing, machine learning, and Bayesian and Monte Carlo inference.